Rb-^{129}Xe spin-exchange rates due to binary and three-body collisions at high Xe pressures

G. D. Cates, R. J. Fitzgerald, A. S. Barton, P. Bogorad,
M. Gatzke, N. R. Newbury, and B. Saam
Department of Physics, Princeton University, Princeton, New Jersey 08544
(Received 24 October 1991)

We have studied the spin relaxation of ^{129}Xe nuclei due to collisions with Rb atoms at Xe pressures of 245–1817 Torr. Our results can be characterized by two parameters, the Rb-^{129}Xe velocity-averaged binary spin-exchange cross section $\langle\sigma v\rangle$ and a rate γ_M that characterizes spin relaxation due to van der Waals molecules. Our results complement earlier studies performed at Xe pressures of about 1 Torr and N_2 pressures of 10–100 Torr. This work is useful for predicting spin-exchange rates between polarized Rb atoms and ^{129}Xe nuclei.

PACS number(s): 32.80.Bx, 33.25.Bn, 34.90.+q

I. INTRODUCTION

There are two mechanisms whereby the nuclei of noble gases can be polarized by spin exchange with optically pumped alkali-metal vapor: binary collisions and the formation of loosely bound van der Waals molecules. A van der Waals molecule is formed by the collision of an alkali-metal atom, a noble-gas atom, and a third body. The first comprehensive theoretical treatment of spin exchange in van der Waals molecules was given by Happer *et al.* [1], and subsequent measurements by Zeng *et al.* [2] confirmed most aspects of the theory. The spin-exchange rates due to van der Waals molecules can be very fast, particularly between alkali-metal atoms and some of the heavier noble gases, such as Kr and Xe. The fast rates make it possible to obtain large nuclear polarizations after several minutes of optical pumping with a laser. Early experiments that took advantage of these high rates include searches for permanent electric dipole moments [3], the measurement of the magnetic moments of various radioactive nuclei [4–6], and the study of coherent quadrupolar wall interactions [7].

Recently, we have become interested in polarizing relatively high pressures of Xe, ranging from several hundred Torr up to several thousand Torr. (Our quoted pressures are understood to be measured at room temperature and thus indicate the density of the gas.) Motivations within our group and elsewhere include the study of spin-polarized xenon ice [8], studies of ^{129}Xe adsorbed on surfaces [9], and the possibility of polarized nuclear targets [10]. At high Xe pressures, there are two aspects of spin exchange that differ markedly from the experiments of Zeng *et al.* [2], where the samples contained about 1 Torr of Xe and 10–100 Torr of N_2. First, for Xe pressures greater than about 350 Torr, the spin-exchange rate due to binary collisions exceeds the spin-exchange rate due to the formation of van der Waals molecules. In the work of Zeng *et al.*, the rate of spin exchange due to binary collisions was negligible. Second, when most of the gas in a sample is Xe, RbXe van der Waals molecules are formed predominantly in collisions with another Xe atom as the third body, in contrast to the experiments of Zeng *et al.*, where RbXe molecules were formed mostly in collisions with N_2 molecules. The work of Zeng *et al.* is thus of limited practical value for the purposes of predicting spin-exchange rates under conditions of high Xe pressure. Our studies therefore complement earlier experiments and provide useful data for characterizing spin-exchange interactions.

According to the theory developed by Happer *et al.* [1], the longitudinal spin-relaxation rate $1/T_1$ of ^{129}Xe in a high-pressure sample containing only Xe and Rb vapor has the simple form

$$\frac{1}{T_1} = [\mathrm{Rb}]\left(\frac{\gamma_M \zeta}{[\mathrm{Xe}]} + \langle\sigma v\rangle\right) + \Gamma', \tag{1}$$

where [Rb] is the number density of Rb, [Xe] is the number density of Xe (all isotopes), $\langle\sigma v\rangle$ is the velocity-averaged binary spin-exchange cross section, Γ' is the relaxation rate due to wall collisions and perhaps magnetic field inhomogeneities [11], and γ_M is a constant. The factor ζ was nearly constant in our work and depends on the nuclear spin and relative abundance of each isotope of Rb. We will discuss ζ later in connection with (7). Note that the molecular and binary spin-exchange contributions to the relaxation in (1) have different pressure dependences. Relaxation occurring in RbXe van der Waals molecules is inversely proportional to [Xe] and is characterized by the rate γ_M. Relaxation due to binary collisions is independent of [Xe] and is proportional to $\langle\sigma v\rangle$.

We measured $1/T_1$ as a function of [Rb] in each of four cells, ranging in Xe pressure from 245–1817 Torr. We fit our results to (1) and extracted values for both γ_M and $\langle\sigma v\rangle$, neither of which has been measured previously.

II. THEORY

The spin Hamiltonian for the Rb-^{129}Xe system in an applied magnetic field $\mathbf{B} = B_z\hat{\mathbf{z}}$ is

$$H = A\mathbf{I}\cdot\mathbf{S} + \gamma\mathbf{N}\cdot\mathbf{S} + \alpha\mathbf{K}\cdot\mathbf{S} + g_S\mu_B\mathbf{B}\cdot\mathbf{S} + \cdots, \quad (2)$$

where $A\mathbf{I}\cdot\mathbf{S}$ is the hyperfine interaction between the Rb valence electron spin $\mathbf{S}$ and its own nuclear spin $\mathbf{I}$, $\gamma\mathbf{N}\cdot\mathbf{S}$ is the spin-rotation interaction between $\mathbf{S}$ and the rotational angular momentum $\mathbf{N}$ of the RbXe system, $\alpha\mathbf{K}\cdot\mathbf{S}$ is the isotropic magnetic dipole interaction between $\mathbf{S}$ and the nuclear spin $\mathbf{K}$ of the Xe, and $g_s\mu_B\mathbf{B}\cdot\mathbf{S}$ is the largest of the Zeeman terms. The term $\alpha\mathbf{K}\cdot\mathbf{S}$ is responsible for spin exchange in the RbXe system. The spin-rotation interaction $\gamma\mathbf{N}\cdot\mathbf{S}$ is the primary cause of the spin relaxation of optically pumped Rb vapor in the RbXe system, and has been measured previously by Bouchiat, Brossel, and Pottier [12]. The ratio $x = \gamma N/\alpha$, referred to as the Breit-Rabi field parameter by Happer and co-workers [1,2], determines the efficiency with which angular momentum can be transferred from Rb atoms to ^{129}Xe nuclei. For each unit of angular momentum lost by a Rb atom during a collision with a ^{129}Xe atom, on average, a fraction equal to $1/x^2$, or $\sim$10%, will be transferred to the ^{129}Xe nucleus.

For binary collisions, it is possible to characterize the spin-exchange rate by a velocity-averaged binary spin-exchange cross section $\langle\sigma v\rangle$. Spin exchange that occurs in molecules, however, is characterized by a three-step process that includes the formation of the van der Waals molecule during a three-body collision, the evolution of the spins during the lifetime of the molecule, and finally, the collisional breakup of the molecule. It is thus convenient to describe the evolution of the nuclear spins by a rate equation. In addition to the parameters that appear in (2), the rate equation includes both the formation rate of van der Waals molecules and their mean molecular lifetime τ.

A. The short molecular lifetime limit

Our high-pressure experiments, for which $P(\mathrm{Xe}) \geq 245$ Torr, are best described by the short molecular lifetime limit for which

$$\left(\frac{\gamma\tau}{(2I+1)\hbar}\right)^2 \ll 1. \quad (3)$$

There are three terms in the rate equation which governs the time evolution of the longitudinal nuclear spin polarization $\langle K_z\rangle$ in this limit. Equation (109) of Happer *et al.* [1] gives the term for molecular spin exchange. To this we add the contribution from binary collisions found in Eq. (123) of Happer *et al.* We emphasize that the relaxation rate given in this equation may be represented by a velocity-averaged spin-exchange cross section times the Rb number density [Rb],

$$[\mathrm{Rb}]\langle\sigma v\rangle = \frac{1}{2}\frac{1}{T_{K'}}\left(\frac{\alpha\tau}{\hbar}\right)^2, \quad (4)$$

where $1/T_{K'}$ is the binary collision rate per noble-gas molecule. Finally, we account for relaxation in the absence of Rb, due to wall collisions and perhaps magnetic field inhomogeneities, with an empirical relaxation rate Γ' and obtain

$$\frac{d}{dt}\langle K_z\rangle = \frac{1}{T_K}\sum_{i=1}^{2} f_i\left(\frac{\alpha\tau}{(2I_i+1)\hbar}\right)^2\left[\langle\hat{K}^2 - K_z^2\rangle\langle F_{iz}\rangle - \langle\hat{F}_i^2 - F_{iz}^2\rangle\langle K_z\rangle\right]$$
$$+[\mathrm{Rb}]\langle\sigma v\rangle\left[2\langle S_z\rangle\langle\hat{K}^2 - K_z^2\rangle - \langle K_z\rangle\right] - \Gamma'\langle K_z\rangle, \quad (5)$$

where $1/T_K$ is the formation rate of van der Waals molecules per noble-gas atom. We have also introduced the operator $\mathbf{F}$, the total angular momentum of the Rb atom, and the notation $\hat{F}^2 = \mathbf{F}\cdot\mathbf{F}$. The summation in the first term is over the two stable isotopes, ^{85}Rb ($I_1 = \frac{5}{2}$) and ^{87}Rb ($I_2 = \frac{3}{2}$), which occur naturally with isotopic fractions $f_1 = 0.7215$ and $f_2 = 0.2785$, respectively.

While (5) is in general complicated, it becomes much simpler for our experiment, in which the nuclear polarization of the ^{129}Xe is decaying in the presence of essentially unpolarized Rb vapor. Under our experimental conditions we expect a spin temperature equilibrium for the Rb vapor [1]. The populations of the spin states of the Rb atom are then weighted by the factor $e^{-\beta(\mathrm{Rb})m_F}$ where $\beta(\mathrm{Rb})$ is a dimensionless quantity proportional to the inverse spin temperature and m_F is an eigenvalue of the longitudinal spin F_z. In the high spin temperature and therefore zero polarization limit, $\langle F_{iz}\rangle = 0$ and $\langle S_z\rangle = 0$. We also use the limit

$$\lim_{\beta(\mathrm{Rb})\to 0}\langle\hat{F}_i^2 - F_{iz}^2\rangle = \frac{1}{2} + \frac{2}{3}I_i(I_i+1). \quad (6)$$

It follows that the sum in (5) no longer depends on $\langle F_{iz}\rangle$, and can be computed explicitly. To simplify further analysis we introduce the parameter

$$\zeta = \sum_{i=1}^{2}\frac{f_i\langle\hat{F}_i^2 - F_{iz}^2\rangle}{(2I_i+1)^2} = 0.1791, \quad (7)$$

where the numerical value corresponds to the isotopic composition of natural Rb.

To further simplify (5), we determine the dependence of the molecular spin-exchange term on the Rb and Xe pressures. From the principle of detailed balance, the formation and breakup rates per unit volume of Rb^{129}Xe van der Waals molecules, given by $[^{129}\mathrm{Xe}]/T_K$ and $[\mathrm{Rb}^{129}\mathrm{Xe}]/\tau$, are equal. Furthermore, these quantities are related to a single pressure-independent rate constant Z:

$$\frac{[^{129}\mathrm{Xe}]}{T_K} = \frac{[\mathrm{Rb}^{129}\mathrm{Xe}]}{\tau} = Z[\mathrm{Rb}][^{129}\mathrm{Xe}][\mathrm{Xe}]. \quad (8)$$

Here we are using brackets around a species to denote its number density. Note that $[^{129}\mathrm{Xe}]$ appears because

$1/T_K$ of (5) is the formation rate per ^{129}Xe atom, while [Xe] appears as the third-body density. Using (8) we can express

$$\frac{1}{T_K}\left(\frac{\alpha\tau}{\hbar}\right)^2 = \frac{[\mathrm{Rb}]}{[\mathrm{Xe}]}\left(\frac{\alpha}{\hbar}\right)^2\left(\frac{[\mathrm{Rb}^{129}\mathrm{Xe}]}{[\mathrm{Rb}][^{129}\mathrm{Xe}]}\right)^2\frac{1}{Z}. \quad (9)$$

Noting that the definition for the chemical equilibrium constant κ is

$$\kappa = \frac{[\mathrm{RbXe}]}{[\mathrm{Rb}][\mathrm{Xe}]} = \frac{[\mathrm{Rb}^{129}\mathrm{Xe}]}{[\mathrm{Rb}][^{129}\mathrm{Xe}]}, \quad (10)$$

where the second equality is true because the van der Waals interaction is independent of nuclear species, we write

$$\frac{1}{T_K}\left(\frac{\alpha\tau}{\hbar}\right)^2 = \frac{[\mathrm{Rb}]}{[\mathrm{Xe}]}\frac{\alpha^2\kappa^2}{\hbar^2 Z} = \frac{[\mathrm{Rb}]}{[\mathrm{Xe}]}\gamma_M, \quad (11)$$

where $\gamma_M = \alpha^2\kappa^2/\hbar^2 Z$ is the constant introduced in (1). When samples contain N_2 as well as Xe, which was the case in our work, we must modify (11) slightly to be

$$\frac{1}{T_K}\left(\frac{\alpha\tau}{\hbar}\right)^2 = \frac{[\mathrm{Rb}]}{[\mathrm{Xe}]}\gamma_M\left(\frac{1}{1+br}\right), \quad (12)$$

where $r = P(N_2)/P(\mathrm{Xe})$ is the ratio of the N_2 pressure $P(N_2)$ to the Xe pressure $P(\mathrm{Xe})$, and the coefficient $b = 0.275$ is a constant. The correction factor $1/(1+br)$, first introduced by Schaefer, Cates, and Happer [13], differs from unity by at most 5% in our experiments, and will be discussed more in Appendix A.

The low Rb polarization limit of (5) can thus be written with the help of (7) and (12) as

$$\frac{d}{dt}\langle K_z\rangle = -\left\{[\mathrm{Rb}]\left[\frac{\gamma_M\zeta}{[\mathrm{Xe}]}\left(\frac{1}{1+br}\right)+\langle\sigma v\rangle\right]+\Gamma'\right\}\langle K_z\rangle. \quad (13)$$

This is the equation to which we fit our experimental data.

B. The very short molecular lifetime limit

The short molecular lifetime limit in (3) is distinct from the *very* short molecular lifetime limit

$$\frac{A\tau(2I+1)}{2\hbar} \ll 1. \quad (14)$$

In this limit (5) is replaced by

$$\frac{d}{dt}\langle K_z\rangle = \frac{1}{2}\frac{1}{T_K}\left(\frac{\alpha\tau}{\hbar}\right)^2\left[2\langle\hat{K}^2-K_z^2\rangle\langle S_z\rangle-\langle K_z\rangle\right] + [\mathrm{Rb}]\langle\sigma v\rangle\left[2\langle S_z\rangle\langle\hat{K}^2-K_z^2\rangle-\langle K_z\rangle\right] - \Gamma'\langle K_z\rangle. \quad (15)$$

The only difference between (15) and (5) is that the molecular term now has a simpler form given by Eq. (123) of Happer *et al.* [1]. This is because the hyperfine interaction is now slow compared to the molecular lifetime. Thus $\langle F_{iz}\rangle$ and $\langle F_i^2 - F_{iz}^2\rangle$ no longer appear, and the Rb polarization is described entirely by $\langle S_z\rangle$. In the limit of low Rb polarization (15) still reduces to the form given by (13) with the caveat that $\zeta = 1/2$.

Our highest pressure cell falls in the transition region in which the ratio in (14) is about 1. The value of ζ in (13) appropriate for this cell is presumably between 0.1791 and 1/2. We will ignore this complication for the present, however, because it has only a minor effect on the interpretation of our data as we will show later.

III. EXPERIMENT

A. Apparatus and method

A schematic of some of the key components of the experimental apparatus is shown in Fig. 1. Measurements were made on four sealed Pyrex cells that each contained about 50 Torr of N_2, several milligrams of natural Rb, and 245–1817 Torr of Xe, isotopically enriched to a fraction of 0.73 ± 0.01 ^{129}Xe. The cells were heated in an oven to temperatures between 75°C and 120°C to achieve Rb number densities between 1.0×10^{12} and 2.0×10^{13} cm^{-3}, respectively. A static magnetic field of 0.11 G was produced along the z axis (see Fig. 1) by a solenoid. Two concentric μ-metal shields were used to reduce the field fluctuations to less than 1 mG, and a Cs magnetometer detected the magnitude of the field. Any fluctuations in the field were canceled by feedback of current into a pair of compensating coils.

The techniques used to fabricate our cells were similar in many respects to the techniques used by Zeng *et al.* [2] with some changes to produce the higher pressures. Each cell was initially attached to a glass manifold by a small stem. After the cell was filled with gas, the stem was heated while simultaneously pulling the cell, causing the stem to collapse and make a seal. Clearly, the gas pressure within a cell must be less than 1 atm while it is sealed, otherwise the internal pressure would blow a leak in the glass when it is hot. For this reason, the Xe was kept frozen while sealing the cell. In order to regulate the

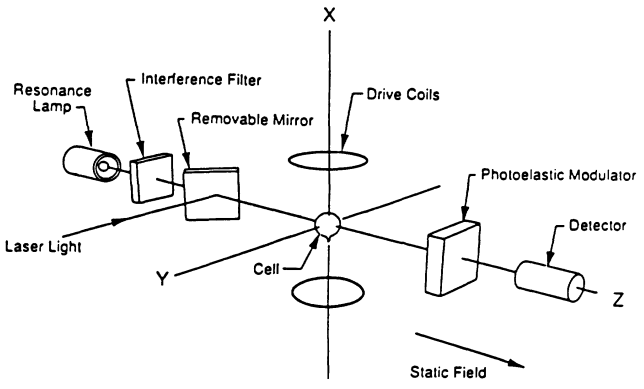

FIG. 1. A schematic of the apparatus is shown, emphasizing the components used to monitor the polarization. Not shown are the magnetic shielding, the solenoid that creates the indicated magnetic field, and the components involved in locking the magnetic field.

amount of Xe in each cell, we measured the volume of our gas manifold, thus making it possible to determine the amount of Xe in the manifold by measuring a pressure. When preparing to seal the cell, we submerged it in liquid nitrogen and monitored the pressure in the manifold to determine the amount of gas that had been frozen. This technique minimized the waste of expensive isotopically enriched Xe. After freezing the desired quantity of Xe in the cell, it was filled with N_2 while still submerged in liquid nitrogen. The filling pressure of N_2 was chosen to be a factor of 77 K/296 K less than the desired final pressure to account for the temperature difference between the cell and the gas manifold.

During the experiment, the cells were heated in order to achieve the desired Rb number density, and the Rb vapor was polarized by optical pumping with a cw dye laser. We used a Coherent 599 broadband dye laser (operated with an LD-700 dye) which was pumped by a Spectra-Physics krypton-ion laser. The ^{129}Xe became polarized by spin-exchange in Rb^{129}Xe van der Waals molecules and binary spin-exchange collisions with polarized Rb atoms. After about 4–10 min substantial polarization was achieved in the ^{129}Xe nuclei, and the laser light was blocked.

To measure the decay of polarization, the sample was probed with the unpolarized 794.8 nm D1 light from a Rb resonance lamp. The Rb vapor became slightly repolarized by spin exchange with the polarized ^{129}Xe nuclei. A photoelastic modulator was used to detect the small amount of circular polarization that was induced in the probe light as it passed through the sample [2]. The probe light was focused onto a photodiode, which was the input for a lock-in amplifier. The resulting signal was proportional, up to an offset, to the longitudinal nuclear spin of the ^{129}Xe atoms. The offset, presumably caused by small amounts of stray circular polarization due to the lamp and other optical components, drifted with time scales that were relatively short compared to the decay times of our polarized samples. To compensate for these small, unpredictable drifts in our output signal, we periodically reversed the polarization of our sample by the application of a resonant, homogeneous oscillating magnetic field along the x axis, induced by the drive coils of Fig. 1. The pulse caused Rabi precession, and the amplitude and duration of the pulse were adjusted to exactly flip the spins of the ^{129}Xe nuclei by 180°. We will refer to this method as π pulsing. Several examples of our raw signals are shown in Fig. 2. The relative Xe polarization was determined by comparing the average signal immediately before and after the inversion. An Apple II+ computer was used to control the entire π-pulsing process and to digitize and store the data. Following each run, the computer fitted the lock-in signal to a simple exponential decay from which we extracted a decay constant. In Fig. 3, we show the ^{129}Xe polarization as a function of time, together with a fit to an exponential decay.

One complication of our technique arises from small losses incurred during the spin inversion. If the oscillating magnetic field is slightly off resonance or if the field is not turned on for the proper amount of time, each spin flip causes a slight loss of polarization. The signal amplitude is thus given by

$$A(t) = A(0)e^{-[1/T_1 - \ln(1-\epsilon)\gamma_F]t}, \tag{16}$$

where ϵ is the spin loss per inversion, γ_F is the the number of spin flips per unit time, and $1/T_1$ is the longitudinal spin-relaxation rate in the absence of the π pulses. The decay constant $1/T'$ that results from a fit like the one in Fig. 3 is thus related to $1/T_1$ by

$$\frac{1}{T'} = \frac{1}{T_1} - \ln(1-\epsilon)\gamma_F. \tag{17}$$

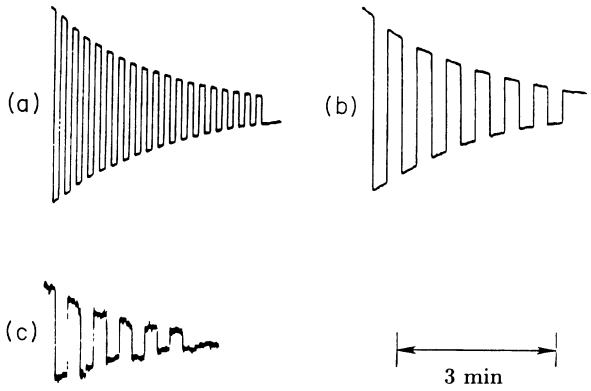

FIG. 2. Raw signals showing the decay of polarization. The polarization of the sample was periodically flipped through an angle of π radians by a pulse of an oscillating magnetic field to remove the effect of offsets and drifts in our signal. (a) and (b) represent runs taken at the same temperature but at different flipping rates. (c) shows, on a more sensitive scale than that in (a) and (b), a signal taken at 115°C, one of the highest temperatures at which we were able to obtain data. The increased noise in (c) is due to the fact that our sample became optically thick to our probe light at elevated temperatures.

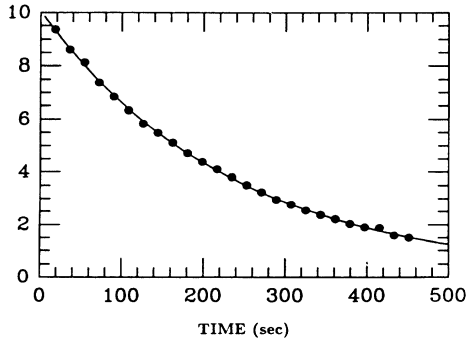

FIG. 3. A typical decay curve, obtained through the analysis of raw signals like those in Fig. 2. Each data point was obtained by comparing the signal immediately before and after the application of a π pulse. The data points and the exponential fit are generated by the Apple II+ computer that controlled the data-taking procedure.

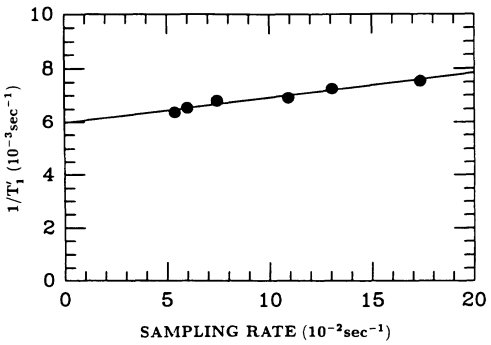

FIG. 4. Exponential decay constants $1/T'$ like the one in Fig. 3 are plotted as a function of the flipping rate. The data are fit to a straight line, and the nonzero slope indicates the losses incurred during the flips. The y intercept of the line is $1/T_1$, the longitudinal spin-relaxation rate of a cell at a particular temperature.

In order to determine $1/T_1$, we measured $1/T'$ five or six times at each temperature, varying the flipping rate during each run. The raw data from typical fast and slow flipping rates are shown in Figs. 2(a) and 2(b), respectively. A plot showing $1/T'$ as a function of the flipping rate γ_F is shown in Fig. 4. The y intercept of this plot is equal to $1/T_1$. We used plots of the sort shown in Fig. 4 both to extract a value for $1/T_1$ and to study the reproducibility of our data. The errors associated with each measurement of $1/T_1$ at a given temperature resulted from consideration of the quality of both the linear fit shown in Fig. 4 and the exponential fit shown in Fig. 3.

B. Results

For each cell, $1/T_1$ was measured as a function of [Rb]. The proper value of [Rb] was maintained by controlling the temperature of the cell and was determined by using the vapor pressure curve measured by Killian [14]:

$$[\mathrm{Rb}] = 10^{(10.55-4132/T)}/kT, \tag{18}$$

where T is the temperature in Kelvin and k is Boltzmann's constant. We varied the temperature of our oven between about 75°C and 120°C. Above 120°C the Rb vapor became so optically thick that our probe was overly attenuated. This resulted in small noisy signals as illustrated in Fig. 2(c), which shows the raw signal from a run taken at 115°C. No data were taken below 75°C, because at lower temperatures very little of the spin relaxation was due to interaction with the Rb.

All of our data are presented in Fig. 5, in which we show four plots of $1/T_1$ versus [Rb] for each of the four cells we measured. Each data point in Fig. 5 is the result of a fit of the sort shown in Fig. 4 and thus represents five or six separate runs. The data shown in Fig. 5 therefore include the results of well over 100 runs.

From (13), we expect the dependence of $1/T_1$ on the Rb number density to be given by

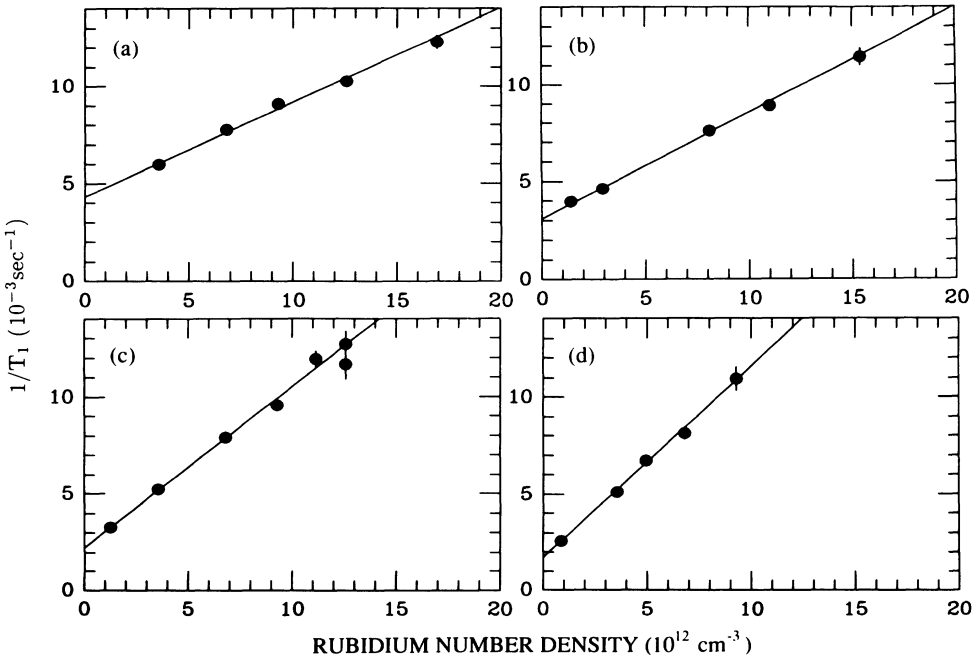

FIG. 5. The longitudinal spin-relaxation rate $1/T_1$ is plotted as a function of the Rb number density [Rb] for each of the four cells we studied. The four plots shown in (a), (b), (c), and (d) correspond to cells 736, 738, 739, and 740, respectively. The data in each plot are fit to a straight line, the slope of which is a measure of γ' as given in (19).

$$\frac{1}{T_1} = [\mathrm{Rb}]\left[\frac{\gamma_M \zeta}{[\mathrm{Xe}]}\left(\frac{1}{1+br}\right) + \langle\sigma v\rangle\right] + \Gamma' = [\mathrm{Rb}]\gamma' + \Gamma'. \tag{19}$$

For convenience we have introduced the parameter γ', the coefficient of [Rb] in (13), which corresponds to the slope of each data set shown in Fig. 5. From (13) we expect that γ' should increase as the pressure in the cells decreases. This trend is clearly evident in the plots shown in Figs. 5(a), 5(b), 5(c), and 5(d), which correspond to Xe pressures of 1817, 843, 350, and 245 Torr, respectively. The y intercept of each plot is the spin-relaxation rate of the ^{129}Xe due to wall collisions and other relaxation mechanisms that do not depend on [Rb]. The results are summarized in Table I.

It is convenient to write the slopes γ' as

$$\gamma' = \left(\frac{\gamma_M \zeta}{2.48 \times 10^{19}\,\mathrm{cm}^{-3}}\right)\frac{1}{P_a} + \langle\sigma v\rangle \tag{20}$$

where

$$\frac{1}{P_a} = \frac{760\,\mathrm{Torr}}{\mathrm{P(Xe)}}\left(\frac{1}{1+br}\right). \tag{21}$$

The dimensionless quantity P_a is essentially the Xe pressure in fractions of an atmosphere, with a small correction factor to account for the presence of N_2. The numerical factor in the denominator on the right-hand side of (20) is the number density of 760 Torr of ideal gas at a temperature of 296 K. Using (20) we can plot γ' as a function of $1/P_a$ and extract values for γ_M and $\langle\sigma v\rangle$. We plot our four measured values of γ' as a function of $1/P_a$ in Fig. 6 and fit the data to a straight line using the method of least squares. From the slope of the line and (20) we obtain

$$\gamma_M = (2.92 \pm 0.18 \pm 0.41) \times 10^4\,\mathrm{sec}^{-1}, \tag{22}$$

where we assume $\zeta = 0.1791$. The first error is due solely to the scatter in the data, and the second error is systematic. From the intercept of Fig. 6, we obtain our value for the velocity-averaged binary spin-exchange cross section of

$$\langle\sigma v\rangle = (3.70 \pm 0.15 \pm 0.55) \times 10^{-16}\,\mathrm{cm}^3\,\mathrm{sec}^{-1}, \tag{23}$$

where again the first error is random and the second error is systematic.

C. The limits of the model

The results (22) and (23) were arrived at under the assumption that all of our data were taken in the short but not very short molecular lifetime regime. While (3) holds for all of our cells, estimates of the left-hand side of (14) based on the measurements of Zeng *et al.* [2] (see also Appendix A) for the four cells are between 1 and 10. Thus, particularly for the highest pressure cell (no. 736), we expect the molecular contribution to spin exchange to exceed the value indicated by (5). Fortuitously, when the pressure becomes high enough that we reach the transition to the very short molecular lifetime regime, the contribution of molecules to spin exchange becomes small compared to that of binary collisions. For example, for cell no. 736 we can use the fitted values given by (22) and (23), and (20) to compute γ' to be $4.58 \times 10^{-16}\,\mathrm{cm}^3\,\mathrm{sec}^{-1}$. The first term in (20), due to van der Waals molecules, is responsible for only 19% of this number. If we use $\zeta = 1/2$ instead of 0.1791, the computed value of γ' climbs by 34% to $6.14 \times 10^{-16}\,\mathrm{cm}^3\,\mathrm{sec}^{-1}$. We measured $4.87 \times 10^{-16}\,\mathrm{cm}^3\,\mathrm{sec}^{-1}$, only 6% higher than our first computed value, and well below the value we expect from using the higher value for ζ. Thus, even our highest-pressure cell fits reasonably well the theoretical form given by (5). We note further that, even if we exclude our highest-pressure data point, our results (22) and (23) change by no more than about 5%. We suggest that (5) is the most expedient interpretation for our observations while cautioning that our model must break down at pressures greater than a few thousand Torr. Most important is that γ' fits well the form given by (20). Taking this view, we have measured the product $\gamma_M \zeta$, which is precisely what is needed for predicting spin-exchange rates.

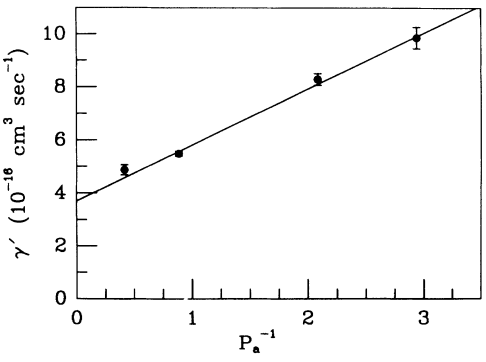

FIG. 6. The measured values of γ' from each cell are plotted as a function of the dimensionless inverse pressure $1/P_a$ given in (21). The data are fit to the straight line given by (20).

TABLE I. Experimental data for each of the four cells.

Cell No.	P(Xe) (Torr)	P(N_2) (Torr)	$1/P_a$	γ' (10^{-16} cm^3 sec^{-1})	Γ' (10^{-3} sec^{-1})
736	1817	50	0.415 ± 0.013	4.87 ± 0.19	4.32 ± 0.14
738	843	49	0.887 ± 0.023	5.48 ± 0.08	3.08 ± 0.05
739	350	52	2.086 ± 0.063	8.28 ± 0.18	2.25 ± 0.08
740	245	49	2.940 ± 0.088	9.85 ± 0.37	1.73 ± 0.14

D. Spin exchange under optical pumping conditions

The [Rb]-dependent part of the longitudinal nuclear spin relaxation of ^{129}Xe in the presence of a Rb vapor is equal to the spin-exchange rate between a polarized Rb vapor and the nuclear spins. Under the assumption of constant Rb polarization and the assumption that $\langle K_z \rangle = 0$ at $t = 0$, we may write a general solution to (5) for spin transfer as

$$\langle K_z \rangle = \langle K_z \rangle_\infty [1 - \exp(-t/T_1)], \tag{24}$$

where $\langle K_z \rangle_\infty$ is the value of $\langle K_z \rangle$ at $t = \infty$ and the spin-transfer rate $1/T_1$ is given by (19). Figure 6 is thus useful for estimating the spin-exchange rate when polarizing ^{129}Xe by spin exchange with a polarized Rb vapor. Knowing the pressure of the cell in atmospheres, one can simply read off a value for γ'. This value, multiplied by the Rb number density, yields the spin-exchange rate. We emphasize, however, that we have made the assumption that the Rb polarization is small.

Under optical pumping conditions, particularly when using a laser, Rb polarizations can be high. In the short molecular lifetime regime, this causes the spin-exchange rate to be somewhat lower than indicated in Fig. 6. We can still compute $1/T_1$ using (19), however, if we reevaluate (7) for the case of higher Rb polarization. With the help of the discussion that appears in Sec. XII of Ref. [1], we see that the limit

$$\lim_{\beta(\mathrm{Rb})\to\infty} \langle \hat{F}_i^2 - F_{iz}^2 \rangle = \frac{1}{2} + I_i. \tag{25}$$

Calculating ζ using (7) in this limit we find for natural Rb that $\zeta = 0.0949$. Thus the full range of ζ in the short molecular lifetime limit is 0.0949–0.1791, corresponding to high and low Rb polarizations. If we consider, for example, a pure Xe sample with $P_a = 0.5$, this yields a range for γ' of $(5.9\text{–}7.9)\times 10^{-16}\,\mathrm{cm^3\,sec^{-1}}$. Note that in the high Rb polarization limit, the contribution to spin exchange from the molecules is roughly half what it is in the low Rb polarization limit.

In the very short lifetime limit (14), $\zeta = 1/2$ and is independent of Rb polarization. We note this for the sake of completeness, since, in this regime, the contribution to $1/T_1$ from molecules is much less than that from binary collisions.

E. The limiting errors of the experiment

The systematic errors quoted in (22) and (23) reflect the extreme sensitivity of the Rb number density to the temperature of the cell. The Rb number density is determined by the coldest spot on the cell. However, the depolarizing effects of magnetic-field inhomogeneities during a nuclear spin flip prevented us from attaching a resistive temperature device (RTD) directly to the cell during our data runs. Instead, the RTD was attached to a point relatively close to the cell, in a location where it did not need to be moved when we changed samples. In order to account for temperature gradients in the oven, we later attached additional RTD's directly to the cell and to several other locations in the oven. These were monitored while the oven temperature was varied over the range in which we took data. We found empirically that the relationship between the cell temperature T_C and the temperature measured by our standard RTD, T_M, was well described by

$$T_C = T_M - a\Delta T, \tag{26}$$

where ΔT is the difference between T_M and the room temperature of about 296 K, and a is a positive constant. Our studies indicated that $a = 0.025 \pm 0.012$. This value of a leads to the conclusion that T_M was 1.3–2.4 K higher than the actual cell temperature. The values of [Rb] used in Fig. 5 were computed using the corrected cell temperature T_C. The temperature correction shifted our final results (22) and (23) by about 20% due to the fact that [Rb] depends on temperature in an exponential fashion. The quoted systematic errors then followed from reanalyzing our data at both limits given by the error in a. Finally, we further increased the errors to account for 10% uncertainties in [Rb] due to uncertainties in Killian's vapor pressure curve (18).

IV. DISCUSSION

The data presented here represent a systematic study of spin relaxation of ^{129}Xe due to interactions with Rb vapor at high Xe pressures. This work complements earlier work by Zeng *et al.* [2] in which Xe pressures of 1 Torr and N_2 pressures of 10–100 Torr were studied. We have shown that the spin relaxation can be characterized by a simple relation containing the two parameters γ_M and $\langle \sigma v \rangle$ that govern the strength of relaxation due to molecules and binary collisions, respectively. We have measured γ_M and $\langle \sigma v \rangle$ at roughly the 15% level. Our measurements are limited by the certainty with which we know the Rb number density as a function of our cell temperature.

Our data make it possible to compute quickly the relaxation rate of polarized ^{129}Xe due to interactions with Rb vapor. The relaxation of ^{129}Xe due to collisions with Rb atoms is given by γ'[Rb], where γ' can either be computed using (19)–(23) or estimated quickly by reading off of the graph in Fig. 6.

While neither γ_M or $\langle \sigma v \rangle$ have been measured previously, an estimate of $\langle \sigma v \rangle$ was given in Eq. (36) of Zeng *et al.* [2] as $\langle \sigma v \rangle = 4.1 \times 10^{-16}\,\mathrm{cm^3\,sec^{-1}}$, which is very close to our measured value. This estimate was based on the measurement of Bouchiat *et al.* [12] of the electron randomization of Rb in the presence of Xe, the theory of Happer *et al.* [1], and the measurement of Zeng *et al.* [2] of the parameter $x = \gamma N/\alpha$. It is much more difficult to estimate γ_M from existing data, but we present two such estimates in Appendix B.

ACKNOWLEDGMENTS

We would like to acknowledge encouragement and many helpful discussions with W. Happer. This work was supported by the U.S. Air Force Office of Scientific Research under Grant No. 88-0165.

APPENDIX A: CORRECTION FOR THE NITROGEN

While most of the gas in our cells is Xe, a small quantity of N_2 is included to aid in optical pumping. If it were not for the N_2, the relaxation of Xe nuclei due to the formation of van der Waals molecules with Rb atoms would be inversely proportional to the Xe pressure. The presence of the N_2 can be accounted for by the factor $1/(1 + br)$ that is introduced in (12). Here $r = P(N_2)/P(Xe)$ is the ratio of the N_2 pressure $P(N_2)$ to the Xe pressure $P(Xe)$. The coefficient $b = P_0(Xe)/P_0(N_2)$, where $P_0(Xe)$ and $P_0(N_2)$ are the characteristic pressures at which the molecular breakup rate τ^{-1} is equal to the spin-rotation frequency $\gamma N/\hbar$ in the limit where only one gas, either Xe or N_2, is responsible for the formation and breakup of the van der Waals molecules. The characteristic pressures are thus defined by

$$\tau = \frac{\hbar}{\gamma N}\frac{P_0}{P}. \tag{A1}$$

The derivation of the factor $1/(1 + br)$ appears in Eqs. (14)–(21) of Ref. [13].

To compute the correction for the presence of N_2, we must know both $P_0(N_2)$ and $P_0(Xe)$. The quantity $P_0(N_2)$ is known from the work of Zeng *et al.* [2], who studied spin exchange between ^{129}Xe and various alkali metals in samples that contained much more N_2 than Xe. The quantity $P_0(Xe)$ has never been directly measured, but it can be inferred by comparing the work of Zeng *et al.* with Bouchiat's studies of the role of van der Waals molecules in the relaxation of polarized Rb atoms in the presence of Xe [12].

In analogy to (8), the molecular lifetime in the experiments of Bouchiat *et al.* and Zeng *et al.* can be related to two rate constants Z_X and Z_N:

$$\begin{aligned}\frac{[Rb]}{T_F} &= Z_X[Rb][Xe][Xe] = \frac{[RbXe]}{\tau},\\ \frac{[Rb]}{T_F} &= Z_N[Rb][Xe][N_2] = \frac{[RbXe]}{\tau},\end{aligned} \tag{A2}$$

where $1/T_F$ is the formation rate of van der Waals molecules per Rb atom. Note that Z_X and Z_N are equivalent to the rate constant Z introduced in (20). We have added the subscripts for clarity and to distinguish between the cases where Xe and N_2 act as the third body during the formation and breakup of van der Waals molecules. From the definition in (A1) of P_0 and (A2), Z and P_0 are both related to the molecular lifetime τ and the equilibrium constant κ of (10), and thus for either experiment,

$$P_0 = \frac{\gamma N}{\hbar}\frac{\kappa}{Z}\frac{P}{[Q]} = \frac{\gamma N}{\hbar}\frac{\kappa}{Z}kT_f, \tag{A3}$$

where [Q] is the density of the third-body gas ([Xe] or $[N_2]$), T_f is the filling temperature, which is room temperature in both experiments, and the second equality results from the ideal gas law. From (A3),

$$\frac{P_0(Xe)}{P_0(N_2)} = \frac{Z_N}{Z_X}. \tag{A4}$$

Zeng *et al.* measured both $P_0(N_2)$ and Z_N which, with the measurement of Bouchiat *et al.* of Z_X, can be used to determine $P_0(Xe)$.

Bouchiat *et al.* measured the Xe pressure dependence of the formation rate of van der Waals molecules when Xe is the third body to obtain

$$T_F P^2(Xe) = (4.29 \pm 0.23) \times 10^{-3}\,\text{sec Torr}^2. \tag{A5}$$

Using (A2), (A5), and the ideal gas law,

$$Z_X = \frac{1}{T_F[Xe]^2} = (2.19 \pm 0.12) \times 10^{-31}\,\text{cm}^6\,\text{sec}^{-1}. \tag{A6}$$

To compare this result with the work of Zeng *et al.*, we must first account for the fact that the two studies were done at different temperatures. If we assume that the breakup cross section of the van der Waals molecules is nearly velocity independent, then we would expect $\tau^{-1} \propto T^{1/2}$. The Boltzman factor $e^{-V/kT}$ (where V is the binding energy of the molecule) does not vary much over the temperature range of interest, so that $\kappa \propto T^{-3/2}$ because of the temperature dependence of the phase space of an ideal gas. Thus, for fixed third-body pressures we write

$$Z = \frac{\kappa\tau^{-1}}{[Q]} \propto T^{-1}. \tag{A7}$$

From (A3) the value of $P_0(Xe)$ can now be given at the temperature T_Z of the experiment of Zeng *et al.* (T_Z = 349 K) in terms of their published values, $P_0(N_2)$ = 103 Torr and $Z_N = 5.1 \times 10^{-32}\,\text{cm}^6\,\text{sec}^{-1}$, as

$$P_0(Xe) = P_0(N_2)\frac{Z_N}{Z_X}\frac{T_Z}{T_B} = 28.3 \pm 4.2\,\text{Torr}, \tag{A8}$$

where T_B = 296 K is the temperature at which Bouchiat *et al.* performed their measurements. To determine the temperature dependence of $P_0(Xe)$, we note $P_0 \propto \tau\gamma N$ from (A1). We expect that γN depends only very weakly on temperature [15], from which we would expect that $P_0 \propto T^{-1/2}$. Therefore

$$P_0(Xe) = (28.3 \pm 4.2\,\text{Torr})\left(\frac{349\,\text{K}}{T}\right)^{1/2}. \tag{A9}$$

APPENDIX B: ESTIMATES OF γ_M

It is possible to estimate a value for γ_M by combining some of the results of Bouchiat *et al.* [12] with those of Zeng *et al.* [2]. First we note that γ_M can be written as

$$\begin{aligned}\gamma_M &= \frac{1}{T_F}\left(\frac{\alpha\tau}{\hbar}\right)^2 = \frac{1}{T_F}\left(\frac{\gamma N\tau}{\hbar}\right)^2\left(\frac{\alpha}{\gamma N}\right)^2\\ &= \frac{1}{T_F}\left(\frac{P_0(Xe)}{P(Xe)}\right)^2\frac{1}{x^2},\end{aligned} \tag{B1}$$

where in obtaining the right-hand side we are making use

of (A1) and the Breit-Rabi field parameter $x = \gamma N/\alpha$ that was measured by Zeng *et al.* as $x = 3.2 \pm 0.3$ for the RbXe system. Using (A6), (A9), and remembering to scale as in (A7), we find that

$$\gamma_M = \left(Z_X[\mathrm{Xe}]^2 \frac{296\,\mathrm{K}}{T}\right)\left(\frac{349\,\mathrm{K}}{T}\right)\left(\frac{28.3\,\mathrm{Torr}}{P(\mathrm{Xe})}\right)^2 \frac{1}{x^2}$$
$$= (1.823 \times 10^4\,\mathrm{sec}^{-1})\frac{(296\,\mathrm{K})(349\,\mathrm{K})}{T^2}. \quad \text{(B2)}$$

The mean temperature at which we made our measurements was about 368 K, so we obtain

$$\gamma_M = (1.39 \pm 0.61) \times 10^4\,\mathrm{sec}^{-1}. \quad \text{(B3)}$$

It is also possible to estimate γ_M by using Eq. (26) of Schaefer, Cates, and Happer [13],

$$\gamma_M = \left(\frac{3}{2}(2I_i + 1)\frac{1}{x^2}\right)\mathfrak{a}_i^*, \quad \text{(B4)}$$

where $\mathfrak{a}_i^*$ is defined by Bouchiat *et al.* [12] as the high-pressure low-magnetic-field limit of the slowest spin-relaxation rate of alkali-metal atoms due to alkali-metal–noble-gas van der Waals molecules. The index i refers to a specific alkali-metal isotope. Using the range $\mathfrak{a}^* = 5000$–$10\,000$ quoted by Bouchiat *et al.* for ^{87}Rb and the measurement of Zeng *et al.* [2] of $x = 3.2 \pm 0.3$ for RbXe van der Waals molecules, we find

$$\gamma_M = (2.34 \pm 1.25) \times 10^4\,\mathrm{sec}^{-1}. \quad \text{(B5)}$$

The discrepancy including errors between γ_M calculated from (B2) and γ_M deduced from our measurements is 1.5 standard deviations. If we use (B4), the discrepancy is 0.4 standard deviations. Our measured value is thus in agreement with the estimates, although both estimates carry roughly 50% uncertainty, which underscores the need for our direct measurement of γ_M.

[1] W. Happer, E. Miron, S. Schaefer, D. Schreiber, W. A. van Wijngaarden, and X. Zeng, Phys. Rev. A **29**, 3092 (1984).

[2] X. Zeng, Z. Wu, T. Call, E. Miron, D. Schreiber, and W. Happer, Phys. Rev. A **31**, 260 (1985).

[3] T. G. Vold, F. Raab, B. Heckel, and E. N. Fortson, Phys. Rev. Lett. **52**, 2229 (1984).

[4] F. P. Calaprice, W. Happer, D. F. Schreiber, M. M. Lowry, E. Miron, and X. Zeng, Phys. Rev. Lett. **54**, 174 (1985).

[5] M. Kitano, M. Bourzutschky, F. P. Calaprice, J. Clayhold, W. Happer, and M. Musolf, Phys. Rev. C **34**, 1974 (1986).

[6] M. Kitano, F. P. Calaprice, M. L. Pitt, J. Clayhold, W. Happer, M. Kadar-Kallen, M. Musolf, G. Ulm, K. Wendt, T. Chupp, J. Bonn, R. Neugart, E. Otten, and H. T. Duong, Phys. Rev. Lett. **60**, 2133 (1988).

[7] Z. Wu, W. Happer, and J. M. Daniels, Phys. Rev. Lett. **59**, 1480 (1987).

[8] G. D. Cates, D. R. Benton, M. Gatzke, W. Happer, K. C. Hasson, and N. R. Newbury, Phys. Rev. Lett. **65**, 2591 (1990).

[9] D. Raftery, H. Long, T. Meersmann, P. J. Grandinetti, L. Reven, and A. Pines, Phys. Rev. Lett. **66**, 584 (1991).

[10] P. A. Souder *et al.*, Los Alamos Meson Production Facility Proposal No. 1164, Los Alamos National Laboratory, 1989 (unpublished).

[11] G. D. Cates, S. Schaefer, and W. Happer, Phys. Rev. A **37**, 2877 (1988).

[12] M. A. Bouchiat, J. Brossel, and L. C. Pottier, J. Chem. Phys. **56**, 3703 (1972).

[13] S. R. Schaefer, G. D. Cates, and W. Happer, Phys. Rev. A **41**, 6063 (1990).

[14] T. Killian, Phys. Rev. **27**, 578 (1926).

[15] Thad G. Walker, Phys. Rev. A **40**, 4959 (1989), and private communication.